Accepted Manuscript

Photodegradation and ecotoxicology of acyclovir in water under UV_{254} and UV_{254} /H_2O_2 processes

Danilo Russo, Antonietta Siciliano, Marco Guida, Emilia Galdiero, Angela Amoresano, Roberto Andreozzi, Nuno M. Reis, Gianluca Li Puma, Raffaele Marotta

PII:	S0043-1354(17)30496-7
DOI:	10.1016/j.watres.2017.06.020
Reference:	WR 12975
To appear in:	*Water Research*
Received Date:	06 March 2017
Revised Date:	05 June 2017
Accepted Date:	07 June 2017

Please cite this article as: Danilo Russo, Antonietta Siciliano, Marco Guida, Emilia Galdiero, Angela Amoresano, Roberto Andreozzi, Nuno M. Reis, Gianluca Li Puma, Raffaele Marotta, Photodegradation and ecotoxicology of acyclovir in water under UV_{254} and UV_{254}/H_2O_2 processes, *Water Research* (2017), doi: 10.1016/j.watres.2017.06.020

Photodegradation and ecotoxicology of acyclovir in water under UV_{254} and UV_{254}/H_2O_2 processes

Danilo Russo[a], Antonietta Siciliano[b], Marco Guida[b], Emilia Galdiero[b], Angela Amoresano[c], Roberto Andreozzi[a], Nuno M. Reis[d,e], Gianluca Li Puma[e,‡] and Raffaele Marotta[a,†]

[a] Dipartimento di Ingegneria Chimica, dei Materiali e della Produzione Industriale, Università di Napoli Federico II, p.le V. Tecchio 80, Napoli, Italy.

[b] Dipartimento di Biologia, Università di Napoli Federico II, Complesso Universitario Monte Sant'Angelo, via Cinthia 4, Napoli, Italy.

[c] Dipartimento di Scienze Chimiche, Università di Napoli Federico II, Complesso Universitario Monte Sant'Angelo, via Cinthia 4, Napoli, Italy.

[d] Department of Chemical Engineering, University of Bath, Claverton Down, Bath BA2 7AY, UK.

[e] Environmental Nanocatalysis & Photoreaction Engineering Department of Chemical Engineering, Loughborough University, Loughborough LE11 3TU, UK.

† *Corresponding author*: Tel.: +39(0)817682968, fax: +39815936936. E-mail address: rmarotta@unina.it (R. Marotta).

‡ *Corresponding author:* Tel.: +44(0)1509222510, fax: +44(0)1509223923. E-mail address: G.Lipuma@lboro.ac.uk (G. Li Puma).

Abstract

The photochemical and ecotoxicological fate of acyclovir (ACY) through UV_{254} direct photolysis and in the presence of hydroxyl radicals (UV_{254}/H_2O_2 process) were investigated in a microcapillary film (MCF) array photoreactor, which provided ultrarapid and accurate photochemical reaction

kinetics. The UVC phototransformation of ACY was found to be unaffected by pH in the range from 4.5 to 8.0 and resembled an apparent autocatalytic reaction. The proposed mechanism included the formation of a photochemical intermediate (ϕ_{ACY} = (1.62 ± 0.07)·10^{-3} mol·ein^{-1}) that further reacted with ACY to form by-products (k' = (5.64 ± 0.03)·10^{-3} $M^{-1}\cdot s^{-1}$). The photolysis of ACY in the presence of hydrogen peroxide accelerated the removal of ACY as a result of formation of hydroxyl radicals. The kinetic constant for the reaction of OH radicals with ACY ($k_{OH/ACY}$) determined with the kinetic modeling method was (1.23 ± 0.07)·10^9 $M^{-1}\cdot s^{-1}$ and with the competition kinetics method was (2.30 ± 0.11)·10^9 $M^{-1}\cdot s^{-1}$ with competition kinetics. The acute and chronic effects of the treated aqueous mixtures on different living organisms (*Vibrio fischeri, Raphidocelis subcapitata*, *D. magna*) revealed significantly lower toxicity for the samples treated with UV_{254}/H_2O_2 in comparison to those collected during UV_{254} treatment. This result suggests that the addition of moderate quantity of hydrogen peroxide (30-150 mg·L^{-1}) might be a useful strategy to reduce the ecotoxicity of UV_{254} based sanitary engineered systems for water reclamation.

Keywords: UVC, hydrogen peroxide photolysis, microreactor, ecotoxicity, water reuse, acyclovir removal.

1. Introduction

Water reclamation and water reuse is becoming increasingly common in industrialized countries with high water demands and in water stressed regions characterized by considerable scarcity of freshwater (Hoekstra, 2014). The most common treatment method for water reuse is chlorination at typical dosages ranging from 5 to 20 mg/L with a maximum of two hours of contact time (Asano, 1998). However, concerns related to (*i*) the adverse impacts of chlorine on irrigated crops, (*ii*) the high ecotoxicity of chlorinated by-products (DBPs) formed during the chlorination stage (Richardson et al., 2007) and (*iii*) the survival of antibiotics resistant bacteria during chlorination

(Khan et al., 2016) with a possible selection of some antibiotic resistance genes in the wastewater microbial community (Huang et al., 2011) should drive the transition from chlorine disinfection to other more ecofriendly suitable methods. UV radiation treatment (especially UVC, $\lambda < 280$ nm) produces a high sterilization efficiency (Montemayor et al., 2008) and could represent a viable alternative to chlorination for the disinfection and reuse of effluents from wastewater treatment plant (WWTP) for irrigation (i.e., after membrane filtration and/or reverse osmosis) or for aquifer recharge. Numerous wastewater sites have adopted UVC treatment for effluents disinfection. For example, Florida and California have favored wastewater reuse and adopted specific regulations on reclamation technologies through UV disinfection processes. UVC doses (fluence) ranging from 50 $mJ \cdot cm^{-2}$ to 150 $mJ \cdot cm^{-2}$ have been suggested to efficiently inactivate pathogens accounting for the variability in the effluent composition (NWRI, 2012), although German and Austrian regulations (DVGW,1997; ONorm, 2001) suggest the use of 40 $mJ \cdot cm^{-2}$ UVC fluence to eliminate a large variety of bacteria and viruses (Conner-Kerr et al., 1998). Even though UV disinfection has been reported highly effective in the reduction of antibiotic resistance bacteria (ARB), particularly in comparison to chlorination (Shi et al., 2013; Hijnen et al., 2006), other investigations have demonstrated that UV disinfection may not contribute to the significant reduction of selected ARB, such as tetracycline-and sulfonamide-resistant bacteria (Munir et al., 2011; Meckes, 1982) thus indicating a plausible selectivity of UV on ARB (Guo et al., 2013).

Moreover, numerous studies have suggested that under the recommended UVC doses several biorefractory xenobiotics, particularly pharmaceuticals and personal care products generally occurring in municipal discharges and partially removed in WWTPs, may undergo photochemical transformations induced by UVC irradiation (Canonica et al., 2008; Nick et al., 1992; Pereira et al, 2007; Kim et al., 2009; Ma et al., 2016; Kovacic et al., 2016; Liu et al., 2016; Marotta et al., 2013) which may generate by-products with high ecotoxicity (Rozas et al., 2016; Yuan et al., 2011). For these reasons, the use of hydrogen peroxide during UVC disinfection (UV_{254}/H_2O_2) which produces highly reactive radical species, has been proposed as a viable treatment for effective removal of

micropollutant and ARB and, in consequence, for the reduction of the ecotoxicity risk (García-Galan et al., 2016; Melo da Silva et al., 2016).

Among the emerging Pharmaceuticals and Personal Care Products detected in WWTP effluents, antiviral drugs play a leading role (Richardson, 2012; Jain et al., 2013) due to their scarce biodegradability (Funke et al., 2016) and increased usage during the last decade, particularly for the treatment of viral diseases and for the prevention of pandemic outbreaks (Hill et al., 2014). Moreover, antiviral drugs have been considered as some of the most hazardous therapeutic substances exerting high toxicity towards biota, such as crustaceans, fish and algae (Sanderson et al., 2004). The presence of antiviral drugs in the environment raises considerable concern regarding their potential effect on the ecosystem, with the potential of developing antiviral drug resistance, in analogy to the development of antibiotic resistant bacteria (Singer et al., 2007; Gillman et al., 2015). Acyclovir (ACY) is one of the oldest and most widely used antiviral drug for treating two common viral infections (chickenpox-zoster and herpes simplex) and it is also prescribed to patients with weakened immune systems in order to control viral infections (i.e., viral conjunctivitis) (Bryan-Marrugo et al., 2015). ACY has been recently detected in different WWTP effluents as well as in surface water at level of few nanograms per liter up to over one micrograms per liter (Table 1).

The photodegradation pathways of ACY under artificial and natural solar light irradiation have been recently investigated (Zhou et al., 2015; Prasse et al., 2015). However, there is a lack of investigations on the photochemical transformation of ACY under UV_{254} and UV_{254}/H_2O_2 treatments and on the simultaneous ecotoxicological assessments of highly diluted treated solutions containing ACY.

More information is needed to determine the effectiveness of UV_{254} assisted processes on the removal of ACY from aqueous solutions and the impact that these processes may have on the structure of aquatic communities and on the ecosystem dynamics.

The use of microcapillary flow photoreactors has recently been proposed to intensify the treatment of substances that are either highly priced, scarcely commercially available or controlled substances

103 such as illicit drugs or selected pharmaceuticals (Reis and Li Puma, 2015; Russo et al., 2016). In
104 contrast to conventional laboratory photochemical systems which require relatively larger volume
105 of liquid, photochemical treatments in microphotoreactors are carried out in a highly controlled
106 environment with minimal sample volumes (of the order of few mL), the sufficient amount to
107 generate samples for subsequent analysis. Furthermore, photochemical transformations in
108 microphotoreactors are executed at extremely short residence times (of the order of seconds) in
109 comparison to conventional laboratory photoreactors, resulting in an efficient use of time and
110 resources.

111 Under this background, in this study we investigated the degradation kinetics of ACY in distilled
112 water under UV_{254} and UV_{254}/H_2O_2 irradiation by means of a microcapillary film (MCF) array
113 photoreactor and we evaluated the acute and chronic ecotoxicity of highly diluted treated samples
114 using a range of selected organisms, to provide important information regarding the photolysis of
115 ACY in UV_{254} based sanitary engineered systems for water reclamation. The toxicity was assessed
116 considering a battery of toxicity tests (*Aliivibrio fischeri*, *Raphidocelis subcapitata*, *Daphnia*
117 *magna*) and endpoints (bioluminescence, growth inhibition, immobilization, survival, reproduction
118 and biomarker) including three trophic and phylogenetic levels (Lofrano et al., 2016).

119 The battery of toxicity tests proposed were sensitive indicators of toxic pollutants, and also
120 determined the great diversity of potential stress-receptor that could result from pharmaceuticals
121 and their byproducts entering the environment (FDA, 1998).

122

123 **2. Materials and methods**

124 *2.1. Materials*

125 Hydrogen peroxide (30% v/v), ACY (pharmaceutical secondary standard), methanol (≥99.9% v/v),
126 formic acid (>99% w/w), benzoic acid (≥99.5% w/w), orthophosphoric acid (85% w/w in H_2O),
127 sodium hydroxide (>98% w/w), perchloric acid (70% v/v), catalase from *Micrococcus lysodeikticus*
128 and reagents for ecotoxicity tests were purchased from Sigma-Aldrich. An aqueous mixture of

129 peptone (32 ppm), meat extract (22 ppm), urea (6 ppm), K_2HPO_4 (28 ppm), $CaCl_2 \cdot H_2O$ (4 ppm),
130 NaCl (7 ppm) and Mg_2SO_4 (0.6 ppm) was used for the preparation of a synthetic wastewater
131 according to the OECD Guidelines (Organisation for Economic Cooperation and
132 development, 1999). The substances were purchased from Sigma-Aldrich and used as received.
133 Milli-Q water was used as solvent in analytical determinations and experiments.
134

135 *2.2. Analytical methods*

136 The concentration of hydrogen peroxide, ACY, and benzoic acid was measured by HPLC (1100
137 Agilent) equipped with a Gemini 5u C6-Phenyl 110 (Phenomenex) reverse phase column and a
138 diode array detector. The mobile phase was a mixture of 93% aqueous orthophosphoric acid (10
139 mM) and 7% methanol flowing at $8.0 \cdot 10^{-4}$ $L \cdot min^{-1}$. The pH of the aqueous solutions was adjusted
140 with NaOH or $HClO_4$ and measured with an Accumet Basic AB-10 pH-meter. The molar
141 absorption coefficient of ACY was estimated using a Perkin Elmer UV/VIS spectrometer (mod.
142 Lambda 35). Total organic carbon (TOC) was monitored by a TOC analyzer (Shimadzu 5000 A).
143 MS analysis was performed by direct injection on Agilent 6230 TOF LC/MS coupled with Agilent
144 HPLC system (1260 Series). The mobile phase was a mixture of methanol (10% v/v) and formic
145 acid (0.1% v/v) aqueous solution at flow rate of 0.4 $mL \cdot min^{-1}$ and the injection volume of samples
146 was 20 µL. The MS source was an electrospray ionization (ESI) interface in the positive ion mode
147 with capillary voltage of 3500 V, gas temperature at 325 °C, dry gas (N_2) flow at 8 $L \cdot min^{-1}$ and the
148 nebulizer at 35 psi. The MS spectra were acquired in a mass range of 100-3000 m/z with a rate of 1
149 spectrum/s, time of 1000 ms/spectrum and transient/spectrum of 9905.
150

151 **3. Experimental apparatus and procedures**

152 *3.1. MCF array photoreactor*

153 The degradation kinetics of ACY by UV_{254} and UV_{254}/H_2O_2 were investigated in a MCF array
154 photoreactor described elsewhere (Reis et al., 2015; Russo et al., 2016). Briefly, the photoreactor

(Lamina Dielectrics Ltd) consisted of ten UV_{254} transparent microcapillaries of fluorinated polymer characterized by a mean hydraulic diameter of 195 μm. The microcapillaries were coiled around a UV monochromatic (254 nm) lamp (Germicidal G8T5) in the region with uniform emission. Experiments were carried out at room temperature (~25 °C) in continuous flow through the reactor at different space times, using capillaries of different length exposed to the UV lamp irradiation. The flow rate through the MCF was $6.0 \cdot 10^{-4}$ $L \cdot min^{-1}$. Aqueous samples were collected from the MCF outlet, and rapidly analyzed by HPLC. At the end of each experimental run, the pH of the solutions was unchanged. The initial concentration of ACY used in the experiments ranged between $2.05 \cdot 10^{-5}$ $mol \cdot L^{-1}$ and $4.67 \cdot 10^{-5}$ $mol \cdot L^{-1}$.

The lamp irradiance was varied by changing the nominal power from 4.5 W to 8.0 W using a variable power supply unit. The photon fluxes per unit volume emitted by the UV lamp (P_o) for each power setting, estimated by H_2O_2 actinometry (Nicole et al, 1990; Goldstein et al., 2007), were $1.92 \cdot 10^{-2}$ $ein \cdot (s \cdot L)^{-1}$ (nominal power 8.0 W) and $1.27 \cdot 10^{-2}$ $ein \cdot (s \cdot L)^{-1}$ (nominal power 4.5 W). The MCF average optical path length (l_{MCF}) was 154 μm. All the runs were carried out in duplicate. The data collected were used to estimate the kinetic unknown parameters (quantum yield of direct photolysis at 254 nm of ACY and kinetic constant of hydroxyl radical attack to ACY).

3.2. Cylindrical batch photoreactor

A cylindrical batch photoreactor (V_b = 0.480 L), equipped with a low-pressure mercury monochromatic lamp (Helios Italquartz, HGL10T5L, 17W nominal power emitting at 254 nm), was used to provide large sample volumes required for the ecotoxicity tests at varying treatment times (i.e., different UV_{254} fluence). The UV_{254} dose ($mJ \cdot cm^{-2}$) was calculated as the average photon fluence rate multiplied by the treatment time. The average photon fluence rate emitted by the UV lamp at 254 nm was 4.7 $mW \cdot cm^{-2}$ (UVC DELTA OHM radiometer). The experimental device was described elsewhere (Spasiano et al., 2016).

180

181 *3.3. Ecotoxicity assessment*

182 Reconstituted aqueous solution (pH =7.8 ± 0.2), was used as dilution water for cladoceran toxicity
183 tests: $CaCl_2 \cdot 2H_2O$ (290 mg·L^{-1}), $MgSO_4 \cdot 7H_2O$ (120 mg·L^{-1}), $NaHCO_3$ (65 mg·L^{-1}), KCl (6
184 mg·L^{-1}). Different salts were used for the preparation of algal test medium: $CaCl_2 \cdot 2H_2O$ (18 mg·L^{-1}),
185 $MgSO_4 \cdot 7H_2O$ (15 mg·L^{1}), NH_4Cl (15 mg·L^{-1}), $MgCl_2 \cdot 6H_2O$ (12 mg·L^{-1}), KH_2PO_4 (1.6 mg·L^{-1}),
186 $FeCl_3 \cdot 6H_2O$ (0.08 mg·L^{-1}), $Na_2EDTA \cdot 2H_2O$ (0.1 mg·L^{-1}), H_3BO_3 (0.185 mg·L^{-1}), $MnCl_2 \cdot 4H_2O$
187 (0.415 mg·L^{-1}), $ZnCl_2$ (0.003 mg·L^{-1}), $CoCl_2 \cdot 6H_2O$ (0.0015 mg·L^{-1}), $Na_2MoO_4 \cdot 2H_2O$ ($7.0 \cdot 10^{-3}$
188 mg·L^{-1}), $CuCl_2 \cdot 2H_2O$ ($1.0 \cdot 10^{-5}$ mg·L^{-1}). Reconstitution solution, osmotic adjusting solution (OAS)
189 and diluent (NaCl 2%) were the reagents used in *Vibrio fischeri* toxicity test (Strategic diagnostics
190 Inc. SDI).

191 The enzymatic assays chosen to evaluate oxidative stress were ROS (reactive oxygen species)
192 content using 2,7- dichlorodihydrofluorescein (H_2DCFDA) and activities of SOD (superoxide
193 dismutase), CAT (catalase) and GST (glutathione transferase) that were measured using respective
194 assay kits according to the manufactorer's instruction's (Sigma Aldrich). All determinations were
195 quantified spectrophotometrically.

196 *V. fischeri*, *R. subcapitata* and acute *D. magna* assays were conducted with an initial ACY
197 concentration of 1.2 mg·L^{-1} and on its related UV_{254} and UV_{254}/H_2O_2 treated solutions. Chronic
198 toxicity and oxidative stress tests on *Daphnia magna* were performed starting on untreated and
199 treated solutions diluted by 100 fold, in order to assess any differences at sub lethal concentration
200 levels. Negative and positive controls were included in each experiment. The significance of
201 differences of toxicity between the treated samples and controls was assessed by the analysis of
202 variance (ANOVA) considering a significance threshold level always set at 5%. For higher variance
203 than 5%, post-hoc tests were carried out with Dunnett's method and Tukey's test. Whenever

possible, toxicity was expressed as median effective concentration (EC_{50}) with 95% confidence limit values. Otherwise, toxicity was expressed as percentage of effect (PE, %).

3.3.1. Organisms maintenance and monitoring

Freeze-dried *Vibrio fischeri* (strain NRRL-B-11177) cells were reconstituted with reagent diluent at 4 °C. *Raphidocelis subcapitata* were cultured in ISO medium (ISO, 2012) at 23 ± 2 °C with continuous 4500 lux light and aeration (0.2 mm filtered air). *Daphnia magna* were cultured at 20 ± 1 °C, with a 16:8 light/dark photoperiod in ISO water (ISO, 2012).

Luminescence *V. fischeri* measurements were performed with Microtox® Model 500 Toxicity Analyzer from Microbics Corporation (AZUR Environmental) equipped with a 30 well incubated at 15 ± 1 °C and with excitation source at 490 nm wavelength.

R. subcapitata density was determined by an indirect procedure using a spectrophotometer (Hach Lange DR5000) and cuvette (5 cm). *D. magna* viability, mobility and growth were observed with a stereomicroscope (LEICA EZ4-HD).

3.3.2. Bacteria toxicity test

The inhibitory effect of ACY samples on the light emission of *V. fischeri* (strain NRRL-B-11177) was evaluated with the 11348-3:2007 ISO method (ISO, 2007). Tests were carried out on an ACY concentration of 1.2 $mg \cdot L^{-1}$ and on its related treated by-products solutions. OAS was added to each sample to ensure that the final NaCl concentration was above 2.0%. The initial light output from each cuvette containing reconstituted freeze-dried *V. fischeri* was recorded. The test solutions were then added and after 30 minutes exposure, the final light output was measured. Positive control tests for *V. fischeri* were carried out with $C_6H_4Cl_2O$ (EC_{50} = 4.1± 2.2 $mg \cdot L^{-1}$).

3.3.3. Algae toxicity test

229 The *R. subcapitata* bioassay was conducted following the guidelines ISO 8692 (ISO, 2012). Three
230 replicates were included for each sample. The replicates were inoculated with 10^4 algal cells·mL^{-1}
231 and incubated for 72 h at 23 ± 2 °C under continuous illumination (irradiance range of 120-60
232 µein·m^{-2}·s^{-1}). The algal biomass exposed to the samples was compared with the algal biomass in the
233 negative control. Positive control tests for *R. subcapitata* were carried out with $K_2Cr_2O_7$ (EC_{50} = 1 ±
234 0.2 mg·L^{-1}).
235
236 *3.3.4. Crustaceans toxicity test*
237 Acute toxicity tests with *D. magna* were carried out according to ISO 6341 (ISO, 2013). Newborn
238 daphnids (<24 h old) were exposed in four replicates for 24 h and 48 h at 20 ± 1 °C. Toxicity was
239 expressed as percentage of immobilized organisms. Positive control tests for *D. magna* were carried
240 out with $K_2Cr_2O_7$ (48h, EC_{50} = 0.6 ± 0.1 mg·L^{-1}).
241 The *D. magna* chronic bioassay was carried out according to the guideline OECD 211 (OECD,
242 2012). Ten *D. magna* neonates (< 24 h hold) were used and individually placed for each treatment
243 in beakers containing 50 ml of the test solutions, renewed every two other days. Organisms exposed
244 for 21 days with ACY solutions were then fed one day with *R. subcapitata* (10^7 cell·mL^{-1}).
245 Survival, reproduction and growth were observed daily, and newborns were discarded from
246 beakers.
247 The amount of ROS produced in *D. magna* was determined using 2,7-dichlorodihydrofluorescein
248 (H_2DCFDA, Sigma Aldrich) using the method previously reported (Galdiero et al., 2016). After 48
249 h of exposure, each exposed and not exposed living daphnids were rinsed with deionized water to
250 remove any excess pharmaceuticals adhered to their body surface and transferred to a 96-well plate.
251 A selected volume (200 µL) of 10 mM H_2DCFDA was added to each well and the plate was then
252 incubated for 4 h in the dark at 20-25°C. Fluorescence was measured using a fluorescence plate

253 reader with an excitation wavelength of 350 nm and an emission of 600 nm. The increase in
254 fluorescence intensity yielded the ROS quantity compared to control.
255 Exposed and not exposed daphnids were homogenized in 1 mL sucrose buffer (0.25 M sucrose, 0.1
256 M Tris-HCl, 1 mM EDTA, pH 7.4) and successively centrifuged at 12.000 g for 15 min at 4°C.
257 Supernatants were collected and used to determinate enzymatic activities. Protein content of the
258 samples was quantified using the protocol described by Bradford (1976) using bovine serum
259 albumin as standard.
260 CAT activity was expressed as H_2O_2 consumed ($U \cdot mg^{-1}$ of protein) to convert it to H_2O and O_2 per
261 minute, per mg protein at 240 nm (Aebi, 1984).
262 SOD activity was calculated by measuring the decrease in the color development of samples at 440
263 nm with the reference to the xantine oxidase/cithocrome method (Crapo et al., 1978). In particular
264 the superoxide radical, generated from the conversion of xanthine to uric acid and H_2O_2 by xanthine
265 oxidase, reacts with the tetrazolium salt WST-1 forming formazan.
266 One unit of SOD was defined as the amount of enzyme required to produce 50% inhibition in the
267 reaction system.
268 GST was calculated by measuring the changes in absorbance recorded at 340 nm due to the
269 conjugation of glutathione to 1-chloro-2,4-dinitrobenzene (Habig et al., 1974).
270 One unit of enzyme was the quantity necessary for the reduction of 1 $\mu mol \cdot L^{-1}$ GSH in 1 min at 37
271 °C.
272 Test runs were performed in triplicate with additional controls including on aqueous solutions
273 containing hydrogen peroxide supplemented with catalase, used to destroy the residual hydrogen
274 peroxide.
275

276 **4. Results and discussion**

277 *4.1. UV_{254} photolysis: kinetic investigation*

The results collected from runs of UV_{254} photolysis of ACY in aqueous solution at three different pH values (4.5, 6.0 and 8.0) in the MCF photoreactor at varying lamp power are reported in Figs. 1a-e as a function of the space time. The results indicate that, for a fixed lamp power, the pH did not affect the conversion. In fact, for these runs a half-time of about 17 seconds was recorded independent of the pH. Moreover, the analysis of the concentration *vs* time profile demonstrated that the photolysis of ACY resembled an apparent autocatalytic behavior which suggested the adoption of an autocatalytic kinetic model to describe the degradation of ACY under the adopted experimental conditions. Since the destruction of guanine based substrates under UV_{254} irradiation has been ascribed to both the direct photolysis of guanine derivatives and the reaction of guanine based molecules with the radical species formed during the photolytic process (Crespo-Hernandez et al., 2000a,b), the simplified reaction scheme (Scheme 1) was considered for the UV_{254} photolysis of ACY, which is a guanine derivative:

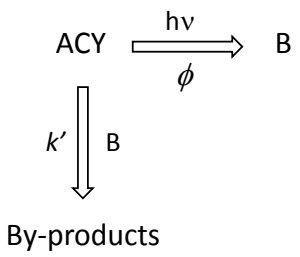

Scheme 1

where B indicates a pseudo intermediate (hydrated electron, oxygen reactive species, etc.) capable of reacting with ACY molecules according to a simple autocatalytic-type kinetics. The quantum yield of photolysis of ACY at 254 nm (ϕ_{ACY}) and the kinetic constant *k'* were estimated through an iterative method, using simultaneously the concentration data reported in Figures 1a,e to solve ODE equations 1 and 2:

$$\frac{d[ACY]}{dt} = -P_o \cdot \emptyset_{ACY} \cdot \left(1 - \exp\left(-2.3 \cdot l_{MCF} \cdot \varepsilon_{254}^{ACY} \cdot [ACY]\right)\right) - k' \cdot [ACY] \cdot [B] \quad (1)$$

$$\frac{d[B]}{dt} = P_o \cdot \emptyset_{ACY} \cdot \left(1 - \exp\left(-2.3 \cdot l_{MCF} \cdot \varepsilon_{254}^{ACY} \cdot [ACY]\right)\right) \quad (2)$$

Where t is the space time in the continuous flow MCF photoreactor (the reaction or exposure time) and the term ε_{254}^{ACY} is the molar absorption coefficient at 254 nm for ACY at pH 4.5, 6.0 and 8.0 ($1.21 \cdot 10^{-2}$ $M^{-1} \cdot cm^{-1}$). This result is in agreement with the pKa values of ACY (2.27 and 9.25) (Florence, 2010).

The MATLAB routine "ode45", based on the Runge-Kutta method with adaptive step-size, was used for the optimization procedure which minimized the objective function $\sum_j^m \sum_i^n \left(y_{ACY_{j,i}} - c_{ACY_{j,i}}\right)^2$, made by the squares of the differences between the calculated "*y*" and experimental "*c*" concentrations of ACY, varying the reaction time "*n*" and for different experimental photolytic runs "*m*". The determined kinetic parameters that minimized the objective function were $\phi_{ACY} = (1.62 \pm 0.07) \cdot 10^{-3}$ $mol \cdot ein^{-1}$ and $k' = (5.64 \pm 0.03) \cdot 10^{-3}$ $M^{-1} \cdot s^{-1}$. The comparison between experimental and calculated data, reported in Figures 1a-e including the percentage standard deviations, demonstrated close prediction of the concentration profiles of ACY in the MCF photoreactor.

The ϕ_{ACY} value reported above has the same order of magnitude as the quantum yield of photodecomposition of other guanine derivatives, such as guanosine and 9-ethyl-guanine at similar concentrations (Crespo-Hernandez et al., 2000a), thus suggesting that the purine structure could play a fundamental role in the UV photolysis of guanine derivatives. The differences could be ascribed to a slight effect of the nature of the group attached to the 9-N on the UV-photolysis kinetics.

4.2. UV_{254}/H_2O_2 oxidation: kinetic investigation

The results of a preliminary run carried out in the presence of hydrogen peroxide under darkness indicated that ACY was not degraded in the presence of H_2O_2 alone for reaction times up to 30 min.

Photooxidation experiments of ACY by the UV_{254}/H_2O_2 process were carried out under the same experimental conditions (i.e., pH, lamp power and initial concentration of ACY) used in the UV_{254} direct photolysis runs.

The degradation profiles for ACY and H_2O_2 as a function of space time in the MCF photoreactor were modeled on the basis of a simplified reaction scheme and the mass balances listed in Table 2. The reaction scheme considers the consumption of ACY and hydrogen peroxide by direct photolysis (*reactions 3 and 4*). Hydroxyl radicals generated by UV_{254} photolysis of H_2O_2 can react with hydrogen peroxide (*reaction 5*), ACY (*reaction 6*) and the transformation products (*reaction 7*). A radical termination of peroxyl radicals was considered in the mechanism (*reaction 8*).

The literature reports two different values of the the kinetic constant of the reaction between hydroxyl radical and ACY ($k_{OH/ACY}$): $5.0 \cdot 10^9$ $M^{-1} \cdot s^{-1}$ (pH=9, T=18 °C, solar simulator $\lambda > 320$ nm) (Prasse et al., 2015) and $1.19 \cdot 10^{10}$ $M^{-1} \cdot s^{-1}$ (pH= 6-9, lamp $\lambda > 340$ nm) (Zhou et al., 2015) which were determined with competition kinetics in the presence of a reference compound (i.e., acetophenone, Zhou et al., 2015, and p-chloro-benzoic acid, Prasse et al., 2015). Since these $k_{OH/ACY}$ values differed by more than 50%, $k_{OH/ACY}$ was determined using both numerical optimization and competition kinetics.

Specifically, the same iterative optimization procedure reported in section 4.1, using simultaneously a set of 9 photodegradation runs in distilled water, at different initial concentrations of ACY and hydrogen peroxide, pH and lamp power, was used for the estimation of $k_{OH/ACY}$. The iterative method minimized the objective function (Eq. 14) that in this case was slightly modified to include the number of the reacting species (h):

$$\Phi = \sum_{g}^{h}\sum_{j}^{m}\sum_{i}^{n}\left(y_{g,j,i} - c_{g,j,i}\right)^2 \tag{14}$$

From this method $k_{OH/ACY}$ was determined as $(1.23 \pm 0.07) \cdot 10^9$ $M^{-1} \cdot s^{-1}$. Graphical examples of the results obtained by the modeling through the optimization procedure are shown in Figures 2a-f

(*optimization procedure*). In Figures 2g-i the comparison is reported between experimental and calculated residual ACY and H_2O_2 concentration, when the model was used in simulation mode without any further parameter adjustment (*simulation mode*), using the $k_{OH/ACY}$ kinetic constant above estimated. It can be noted a good capability of the model of predicting the experimental data under the adopted conditions.

Two additional UV_{254}/H_2O_2 runs (Figs. 2l-m) were carried out using synthetic wastewater to further validate the kinetic results obtained. The photolytic runs were simulated using the proposed kinetic model properly modified to include the HO radical scavenging effect of the species forming the synthetic matrix (Spasiano et al., 2016). For this purpose, the pseudo-first order rate constant (k'_{sca} = $4.01 \cdot 10\ s^{-1}$) was considered for the reaction between the hydroxyl radicals and the scavenger species (Spasiano et al., 2016). Also in this case, a good capability of the model was still observed to predict the experimental data under the adopted conditions.

The competition kinetic method was used to estimate the $k_{OH/ACY}$ constant in the same MCF photoreactor, to further validate the kinetic model proposed above. The method compares the ACY concentration decay to that of benzoic acid (BA) (initial concentration $2.0 \cdot 10^{-5}$ M) chosen as reference compound (Onstein et al., 1999):

$$Ln\left(\frac{[ACY]}{[ACY]_o}\right) = \frac{k_{OH/ACY}}{k_{OH/BA}} \cdot Ln\left(\frac{[BA]}{[BA]_o}\right) \qquad k_{OH/BA} = 5.9 \cdot 10^9 M^{-1} \cdot s^{-1} \quad (pH = 6.0) \qquad (15)$$

An average value $k_{OH/ACY}$ = $(2.30 \pm 0.11) \cdot 10^9\ M^{-1} \cdot s^{-1}$ was thus calculated from UV_{254}/H_2O_2 experiments carried out at pH = 6.0 and $[H_2O_2]_o/[ACY]_o$ = 20 and at different lamp power (4.5 W and 8.0 W). The difference of this from the value estimated with kinetic modeling may be ascribed to the intrinsic limitations of the competition kinetics method that does not include the contribution of ACY consumption by direct photolysis. However, both $k_{OH/ACY}$ values estimated in the present investigation were significantly lower than those previously reported in the literature (Zhou et al., 2015; Prasse et al., 2015).

368 *4.3. UV_{254} photolysis and UV_{254}/H_2O_2 oxidation: Ecotoxicity assessment*

369 A battery of ecotoxicity tests on *V. fischeri*, *D. magna* and *R. subcapitata* were performed on
370 untreated and treated aqueous solutions with an initial ACY concentration of 1.2 $mg \cdot L^{-1}$. The
371 results showed that the inhibition of *V. fischeri* luminescence remained unchanged in the presence
372 of the UV_{254} and UV_{254}/H_2O_2 irradiated solutions, in comparison to the untreated solution (data not
373 shown).

374 The results obtained for *D. magna* (exposure time = 24 and 48 h) for the UV_{254} and UV_{254}/H_2O_2
375 treated and untreated samples are reported in Figures 3A,B. The samples treated with UV_{254}
376 irradiation in the absence of hydrogen peroxide, initially showed an increase of immobility of
377 daphnids at increasing UV_{254} dose and consequently at higher ACY conversion, suggesting an
378 increase in acute ecotoxicity, although, this eventually decreased significantly at the highest UV_{254}
379 dose. On the other hand, the acute ecotoxicity of the UV_{254}/H_2O_2 treated solutions toward *D. magna*
380 was significantly lower in comparison to the samples treated with UV_{254} only, even at much lower
381 UV doses. It is important to note that the acute ecotoxicity of the UV_{254} sample after complete
382 conversion of ACY was higher than the value for the un-irradiated control sample.

383 The inhibition growth of *R. subcapitata* reached 32%, 13% and 20% at UV_{254} doses of 864, 2356
384 and 4712 $mJ \cdot cm^{-2}$ respectively (Fig. 4), thus confirming an acute toxicological effect on the UV_{254}
385 only treated samples. In contrast, a small reduction of the inhibition growth was observed for the
386 samples treated with UV_{254}/H_2O_2 at increasing UV_{254} doses, which supported the beneficial effect
387 of the H_2O_2 assisted photolytic treatment for toxicity reduction.

388 The results showed an increase of the production of ROS in all samples, that could enhance the
389 sublethal toxicity in daphnids. Aquatic organisms can in fact adapt to an increase of ROS
390 production by upregulating the activity of their antioxidant enzymes, particularly of CAT and SOD
391 which represent the first and the second line of defense against ROS (Oexle et al., 2016). An
392 evident increase of ROS production in the daphnids treated with UV_{254} only samples was observed
393 in comparison to the those treated with the UV_{254}/H_2O_2 samples (Fig. 5A). The increase was

recorded for UVC doses of 864 and 2356 mJ·cm^{-2} for the UV_{254} process and at 280 mJ·cm^{-2} for the samples treated with UV_{254}/H_2O_2.

The SOD activity resulted in significant alterations only for samples treated by UV_{254} (Fig. 5B). The enzyme inhibition increased when the UVC dose was increased and reached the highest inhibition at 2356 mJ·cm^{-2}. No effect was observed in the samples treated with UV_{254}/H_2O_2 except for samples treated with a UVC dose of 280 mJ·cm^{-2} (TOC removal degree: 28%).

Both processes led to a significant increase of CAT activity compared to the control (Fig. 5C), since CAT is responsible for the detoxification of high levels of hydrogen peroxide, one of the most important ROS producers under oxidative stress conditions.

On the contrary, GST activity remained unchanged or decreased with both treatments as shown in Figure 5D. Probably the response patterns may be species-specific in nature, while varying in intensity response. The antioxidant enzymes can maintain cellular redox balance, alleviate the toxicological effects of ROS and protect the cells against the oxidative damage of their structures including lipid, membranes, proteins and nucleic acids (Oropesa et al., 2017).

A 21 days chronic exposure experiment was performed to determine the toxicity of 100 fold diluted untreated and treated solutions. The effects of ACY (120 μg·L^{-1}) and its treated samples on *D. magna* reproduction and survival are reported in Figure 6A,B.

The results of chronic toxicity showed that the UV_{254} treatment, even at such low concentrations of ACY, significantly decreased the survival of *D. magna* compared to the control group. A decrease of survival was further recorded for samples exposed at a TOC removal of less than 5% (ACY conversion degree: 45%), probably due the presence of unconverted ACY, and at UV_{254} dose of 2356 mJ·cm^{-2} (ACY conversion: 90%), due to the formation of first-generation-transformation by-products structurally similar to ACY. At higher UV_{254} doses (4712 mJ·cm^{-2}, TOC removal ~ 5%), the survival percentage was similar to that of the control samples and always higher to that of the untreated sample. On the contrary, the ecotoxicity assessment for the UV_{254}/H_2O_2 treated solutions

419 reflected the results already recorded in the acute tests, revealing a marked reduction of chronic
420 toxic effects for the exposures of the daphnids to the UV_{254}/H_2O_2 samples, especially the highest
421 UV_{254} doses (950 mJ·cm^{-2}, TOC removal 77% and 1900 mJ·cm^{-2}, TOC removal higher than 95%).
422 As reported in Table 3, the reproduction of *D. magna* was completely inhibited in the organisms
423 contacted with samples exposed to UV_{254} doses of 864 mJ·cm^{-2} and 2356 and in absence of H_2O_2.
424 These results revealed that all the endpoints were different than the control solutions with an
425 extended exposure to the treatment, thus confirming that the photoproducts formed during UV_{254}
426 irradiation of aqueous ACY solutions exerted significant chronic adverse effects to *D. magna* at the
427 population level. On the contrary, the total number of neonates and the number of first-brood were
428 not statistically different among the samples untreated and treated by UV_{254}/H_2O_2.
429 The different chemical species formed during the UV_{254} and the UV_{254}/H_2O_2 photochemical
430 processes could reasonably explain the observed toxicological effects. To provide a preliminary
431 validation of this hypothesis, two samples, one from UV_{254} photolysis and the second from
432 UV_{254}/H_2O_2 treatment, were directly analyzed with MS-spectrometer to identify the main chemical
433 intermediates formed, with the knowledge that a thorough identification of the transformation by-
434 products required more sophisticated diagnostic techniques (Buchberger, 2011).
435 A list of molecular structures of the main intermediates that could be attributed to some peaks
436 detected in the mass spectra for two samples is reported in Table 4. Some of the structures shown in
437 Table 4 correspond to the chemical intermediates previously detected and reported in literature. In
438 particular, for the UV_{254} photolysis, the structures II, IV and V were observed during the
439 degradation of ACY by TiO_2 photocatalysis at 365 nm (An et al., 2015) whereas the by-products
440 VII and X proposed for UV_{254}/H_2O_2 were the same of those observed during the photooxidation of
441 ACY in phosphate buffer at wavelength higher than 270 nm (Iqbal et al., 2005).. The attribution of
442 reliable structures to the remaining recorded MS signals not previously observed by others, needs
443 further analytical assessments. However, although an uncomplete analysis is available for the
444 products of degradation of ACY, the data collected indicated the presence of chemical species

445 significantly different in the two samples. In particular, UV_{254}/H_2O_2 process seems to lead mainly to
446 the formation of hydroxylated imidazole-based compounds or species formed by the fragmentation
447 of the pyrimidine ring whereas some hydroxylated ACY based intermediates are detected in the
448 UV_{254} treated sample.
449

450 **5. Conclusion**

451 The photodegradation of ACY was investigated under UV_{254} irradiation in the absence and in the
452 presence of hydrogen peroxide. A moderate rate of direct photolysis at 254 nm for ACY was
453 observed with a quantum yield of $(1.62 \pm 0.073)\cdot 10^{-3}$ mol·ein^{-1} in the pH range 4.5 – 8.0. An
454 average value of $1.76\cdot 10^{9}$ $M^{-1}\cdot s^{-1}$ was calculated for the kinetic constant of reaction between
455 hydroxyl radical and ACY. Considering (*i*) the UV_{254} doses typically used for the disinfection of
456 municipal sewage treatment plant effluents, (*ii*) the concentration values of ACY measured in
457 WWTP effluents, and (*iii*) the results collected during the kinetic and ecotoxicity assessment, the
458 occurrence of residual photodecomposition by-products in treated effluents is very likely, and these
459 are likely to have a high ecotoxicological index. However, the addition of appropriate amount of
460 hydrogen peroxide during the UV_{254} disinfection stage would reduce this risk.
461 The results obtained contribute to provide useful information for a vision about the fate of ACY
462 during the UV_{254} and UV_{254}/H_2O_2 treatment processes and the eventual associated risks for living
463 organisms (animals and plants) in the aquatic environment.
464 The results collected confirm the use of oxidative stress biomarkers as promising tool in order to
465 evaluate the toxicological effects of environmental pollutants as early indicators in ecotoxicology.
466 Exposure to environmental pollutants may disrupt the balance of biological oxidant-to-antioxidant
467 ratio in aquatic species leading to elevated levels of ROS and resulting in oxidative stress. A
468 preliminary analysis on the treated samples indicated, as the main photo-transformation by-
469 products, the presence of hydroxylated ACY based intermediates in the UV_{254} treatment process,

and hydroxylated imidazole based compounds or species formed by the fragmentation of the pyrimidine ring in the UV_{254}/H_2O_2 treatment process.

Further efforts are required to identify the main photoproducts, to elucidate the mechanism of ACY photodegradation under UVC radiation and to evaluate possible cumulative effects of the different species occurring in STP effluents.

Acknowledgements

The Authors are grateful to ERASMUS-Mobility Student Program, and to Ing. Giulio Di Costanzo for his precious support during the experimental campaign.

References

Aebi, H., (1984) Catalase in vitro. Methods in Enzymology 6, 105–121.

An, T., An, J., Gao, Y., Li, G., Fang, H., Song, W. (2015) Photocatalytic degradation and mineralization mechanism andtoxicity assessment of antivirus drug acyclovir: Experimental and theoretical studies. Applied Catalysis B: Environmental 164, 279–287.

Asano, T. (1998) Wastewater Reclamation and Reuse, in Water Quality Management Library, Vol 10. C.R.C. Press, Boca Raton.

Azuma, T., Arima, N., Tsukada, A., Hirami, S., Matsuoka, R., Moriwake, R., Ishiuchi, H., Inoyama, T., Teranishi, Y., Yamaoka, M., Mino, Y., Hayashi, T., Fujita, Y., Masada, M. (2016) Detection of pharmaceuticals and phytochemicals together with their metabolites in hospital effluents in Japan, and their contribution to sewage treatment plant influents. Science of the Total Environment 548–549, 189–197.

Bielski, B.H., Cabelli, D.E., Aruda, R.L., Ross, A.B. (1985) Reactivity of HO_2/O_2 radicals in aqueous solution. Journal of Physical and Chemical Reference Data 14, 1041-1077.

Bradford, M.M. (1976) A rapid and sensitive method for the quantitation of microgram quantities of protein utilizing the principle of protein-dye binding. Anal. Biochem. 72, 248–254.

496 Bradley, P.M., Barber, L.B., Duris, J.W., Foreman, W.T., Furlong, E.T., Hubbard, L.E.,
497 Hutchinson, K.J., Keefe, S.H., Kolpin, D.W. (2014) Riverbank filtration potential of
498 pharmaceuticals in a wastewater-impacted stream. Environmental Pollution 193, 173–180.
499 Bryan-Marrugo, O.L., Ramos-Jiménez, J., Barrera-Saldana, H., Rojas-Martínez, A., Vidaltamayo,
500 R., Rivas-Estilla, A.M. (2015) History and progress of antiviral drugs: From acyclovir to direct-
501 acting antiviral agents (DAAs) for Hepatitis C. Medicina Universitaria 17(68), 165–174.
502 Buchberger, W.W. (2011) Current approaches to trace analysis of pharmaceuticals and personal
503 care products in the environment. Journal of Chromatography A 1218, 603–618.
504 Buxton, G.V., Greenstock, C.L., Helman, W.P., Ross, A.B. (1988) Critical review of rate constants
505 for reactions of hydrated electrons, hydrogen atoms and hydroxyl radicals (OH/O) in aqueous
506 solution. Journal of Physical and Chemical Reference Data 17, 513–886.
507 Canonica, S., Meunier, L., von Gunten, U. (2008) Phototransformation of selected pharmaceuticals
508 during UV treatment of drinking water. Water Research 42, 121–128.
509 Conner-Kerr, T.A., Sullivan, P.K., Gaillard, J., Franklin, M.E., Jones, R.M. (1998) The effects of
510 ultraviolet radiation on antibiotic-resistant bacteria in vitro. Ostomy Wound Manage. 44, 50–56.
511 Crapo, J.D., McCord, J.M., Fridovich, I. (1978) Preparation and assay of superoxide dismutases.
512 Methods in Enzymology 53, 382–393.
513 Crespo-Hernandez, C.E., Flores, S., Torres, C., Negron-Encarnacion, I., Arce, R. (2000a) Part I.
514 Photochemical and photophysical studies of guanine derivatives: intermediates contributing to its
515 photodestruction mechanism in aqueous solution and the participation of the electron adduct.
516 Photochemistry and Photobiology 71(5), 534–543.
517 Crespo-Hernandez, C.E., Arce, R. (2000b) Part II. Mechanism of formation of guanine as one of the
518 major products in the 254 nm photolysis of guanine derivatives: concentration and pH effects.
519 Photochemistry and Photobiology 71(5), 544–550.
520 Da Silva, L.M., Cavalcante, R.P., Cunha, R.F., Gozzi, F., Dantas, R.F., De Oliveira, S.C.,
521 Machulek, A.J. (2016) Tolfenamic acid degradation by direct photolysis and the UV-ABC/H2O2

process: factorial design, kinetics, identification of intermediates, and toxicity evaluation. Science of the Total Environment 573, 518–531.

DVGW, 1997. W 294. UV-Desinfektionsanlagen furdie Trinkwasserversorgung-Anforderungen und Prufung.

FDA (Food and Drug Administration). Guidance for Industry: Environmental Assessment of Human Drug and Biologics Application. CDER/CBER CMC 6, rev 1, 39 pp, July 1998. Available: http://www.fda.gov/cber/guidelines.htm.

Florence, A. T. (2010) An Introduction to Clinical Pharmaceutics. Ed. Pharmaceutical Press, London.

Funke, J., Prasse, C., Ternes, T.A. (2016) Identification of transformation products of antiviral drugs formed during biological wastewater treatment and their occurrence in the urban water cycle. Water Research 98, 75–83.

Galdiero, E., Siciliano, A., Maselli, V., Gesuele, R., Guida, M., Fulgione, D., Galdiero, S., Lombardi, L., Falanga, A. (2016) An integrated study on antimicrobial activity and ecotoxicity of quantum dots and quantum dots coated with the antimicrobial peptide indolicidin. International Journal of Nanomedicine 11, 4199–4211.

García-Galan, M. J., Anfruns, A., Gonzalez-Olmos, R., Rodriguez-Mozaz, S., Comas, J. (2016) Advanced oxidation of the antibiotic sulfapyridine by UV/H_2O_2: Characterization of its transformation products and ecotoxicological implications. Chemosphere 147, 451–459.

Gillman, A., Nykvist, M., Muradrasoli, S., Soderstrom, H., Wille, M., Daggfeldt, A., Brojer, C., Waldenstrom, J., Olsen, B., Jarhult, J.D. (2015) Influenza A(H7N9) virus acquires resistance-related neuraminidase I222T substitution when infected mallards are exposed to low levels of oseltamivir in water. Antimicrobial Agents and Chemotherapy 59(9), 5196–5202.

Goldstein, S., Aschengrau, D., Diamant, Y., Rabani, J. (2007) Photolysis of aqueous H_2O_2: quantum yield and applications for polychromatic UV actinometry in photoreactors. Environmental Science & Technology 41, 7486-7490.

Guo, M.T., Yuan, Q.B., Yang, J. (2013) Ultraviolet reduction of erythromycin and tetracyclineresistant heterotrophic bacteria and their resistance genes in municipal wastewater. Chemosphere 93, 2864–2868.

Habig, W.H., Pabst, M.J., Jakoby, W.B. (1974) Glutathione-S-transferases. The first step in mercapturic acid formation. Journal of Biological Chemistry 249, 7130–7139.

Hijnen, W.A.M., Beerendonk, E.F., Medema, G.J. (2006) Inactivation credit of UV radiation for viruses, bacteria and protozoan (oo)cysts in water: a review. Water Research 40 (1), 3–22.

Hill, A., Khoo, S., Fortunak, J., Simmons, B., Ford, N. (2014) Minimum costs for producing hepatitis C direct-acting antivirals for use in large-scale treatment access. Programs in Developing Countries. Clinical Infectious Diseases 58(7), 928–936.

Hoekstra, A.Y. (2014) Water scarcity challenges to business. Nature Climate Change 4, 318–322.

Huang, J.J., Hu, H.Y., Tang, F., Li, Y., Lu, S.Q. Lu, Y. (2011) Inactivation and reactivation of antibiotic-resistant bacteria by chlorination in secondary effluents of a municipal wastewater treatment plant. Water Research 45, 2775−2781.

Iqbal, J., Husain, A., Gupta, A. (2005) Photooxidation of acyclovir in aqueous solution. Pharmazie 60(8), 574–576

ISO 6341:2013 Water quality: determination of the inhibition of the mobility of *Daphnia magna* Straus (Cladocera, Crustacea) acute toxicity test.

ISO 8692:2012 Water quality: fresh water algal growth inhibition test with unicellular green algae.

ISO 11348-3:2007 Water quality: determination of the inhibitory effect of water samples on the light emission of Vibrio fischeri (Luminescent bacteria test), part 3: method using freeze-dried bacteria.

Jain, S., Kumar, P., Vyas, R.K., Pandit, P., Dalai, A.K. (2013) Occurrence and removal of antiviral drugs in environment: A review. Water, Air, & Soil Pollution 224, 1410–1419.

Khan, S., Beattie, T.K., Knapp, C.W. (2016) Relationship between antibiotic- and disinfectant-resistance profiles in bacteria harvested from tap water. Chemosphere 152, 132–141.

Kim, I., Yamashita, N., Tanaka, H. (2009) Photodegradation of pharmaceuticals and personal care products during UV and UV/H_2O_2 treatments. Chemosphere 77, 518–525.

Kovacic, M., Perisic, D.J., Biosic, M., Kusic, H., Babic, S., Bozic, A.L. (2016) UV photolysis of diclofenac in water; kinetics, degradation pathway and environmental aspects. Environmental Science and Pollution Research 23, 14908–14917.

Liu, W.R., Ying, G.G., Zhao, J.L., Liu, Y.S., Hu, L.X., Yao,L., Liang, Y.Q., Tian, F. (2016) Photodegradation of the azole fungicide climbazole by ultraviolet irradiation under different conditions: Kinetics, mechanism and toxicity evaluation. Journal of Hazardous Materials 318, 794–801.

Lofrano, G., Libralato, G., Adinolfi, R., Siciliano, A., Iannece, P., Guida, M., Giugni, M., Volpi Ghirardini, A., Carotenuto, M. (2016) Photocatalytic degradation of the antibiotic chloramphenicol and its by-products toxicity effects. Ecotoxicology and Environmental Safety 123, 65–71.

Ma, J., Lv, W., Chen, P., Lu, Y., Wang, F., Li, F., Yao, K., Liu, G. (2016) Photodegradation of gemfibrozil in aqueous solution under UV irradiation: kinetics, mechanism, toxicity, and degradation pathways. Environmental Science and Pollution Research 23, 14294–14306.

Marotta, R., Spasiano, D., Di Somma, I., Andreozzi, R. (2013) Photodegradation of naproxen and its photoproducts in aqueous solution at 254 nm: a kinetic investigation. Water Research 47, 373–383.

McCurry, D.L., Bear, S.E., Bae, J., Sedlak, D.L., McCarty, P.L., Mitch, W.A. (2014) Superior removal of disinfection byproduct precursors and pharmaceuticals from wastewater in a staged anaerobic fluidized membrane bioreactor compared to activated sludge. Environmental Science& TechnologyLetters 1, 459−464.

Meckes, M.C. (1982) Effect of UV light disinfection on antibiotic-resistant coliforms in wastewater effluents. Appl. Environ. Microbiol. 43, 371–377.

Montemayor, M., Costan, A., Lucena, F., Jofre, J., Munoz, J., Dalmau, E., Mujeriego, R., Salas L. (2008) The combined performance of UV light and chlorine during reclaimed water disinfection. Water Science & Technology 57(6), 935–940.

Munir, M., Wong, K., Xagoraraki, I. (2011) Release of antibiotic resistant bacteria and genes in the effluent and biosolids of five wastewater utilities in Michigan. Water Research 45, 681–693.

Nick, K., Scholer, H.F., Mark, G., Soylemez, T., Akhlaq, M.S., Schuchmann, H.P., von Sonntag, C. (1992) Degradation of some triazine herbicides by UV radiation such as used in the UV disinfection of drinking water. Journal of Water Supply: Research and Technology Aqua 41(2), 82–87

Nicole, I., De Laat, J., Doré, M., Duguet, J.P., Bonnel, C. (1990) Use of UV radiation in water treatment: measurement of photonic flux by hydrogen peroxide actinometry. Water Research 24, 157-168.

NWRI (2012) Ultraviolet Disinfection: Guidelines for Drinking Water and Water Reuse, Third Edition. Published by National Water Research Institute.

OECD (2012) Guidelines for Testing of Chemicals. Daphnia magna Reproduction Test. OECD 211. Paris, France.

Oexle, S., Jansen, M., Pauwels, K., Sommaruga, M., De Meeste,r L., Stoks, R. (2016) Rapid evolution of antioxidant defence in a natural population of *Daphnia magna*. Journal of Evolutionary Biology 29, 1328–1337.

ONorm, M. (2001). Anlagen zur Desinfektion von Wasser mittels Ultraviolett-Strahlen. Anforderungen und Prufung 5873–1.

Onstein, P., Stefan, M.I., Bolton, J.R. (1999) Competition kinetics method for the determination of rate constants for the reaction of hydroxyl radicals with organic pollutants using the UV/H_2O_2 advanced oxidation technology: the rate constants for the tert-buthylformate ester and 2,4-dinitrophenol. Journal of Advanced Oxidation Technologies 4(2), 231–236.

Organisation for Economic Cooperation and development (OECD), 1999. Guidelines for testing of chemicals, simulation test-aerobic sewage treatment, 303A.

Oropesa, A.L., Novais, S.C., Lemos, M.F.L. Espejo, A., Gravato, C., Beltran, F. (2017) Oxidative stress response of *Daphnia magna* exposed to effluents spiked with emerging contaminants under ozonation and advanced oxidation process. Environmental Science & Pollution Research 24, 1735–1747.

Peng, X., Wang, C., Zhang, K., Wang, Z., Huang, Q., Yu, Y., Ou, W. (2014) Profile and behavior of antiviral drugs in aquatic environments of the Pearl River Delta, China. Science of the Total Environment 466–467, 755–761.

Pereira, V.J., Weinberg, H.S., Linden, K.G., Singer, P.C. (2007) UV degradation of pharmaceutical compounds in surface water via direct and indirect photolysis at 254 nm. Environmental Science& Technology 41(5), 1682–1688.

Prasse, C., Schlusener, M.P., Schulz, R., Ternes, T.A. (2010) Antiviral drugs in wastewater and surface waters: A new pharmaceutical class of environmental relevance? Environmental Science & Technology 44, 1728–1735.

Prasse, C., Wagner, M., Schulz, R., Ternes, T.A. (2011) Biotransformation of the antiviral drugs acyclovir and penciclovir in activated sludge treatment. Environmental Science & Technology45(7), 2761–2769.

Prasse, C., Wenk, J., Jasper, J.T., Ternes, T.A., Sedlak, D.L.(2015) Co-occurrence of photochemical and microbiological transformation processes in open-water unit process wetlands. Environmental Science & Technology 49, 14136−14145.

Reis, N.M., Li Puma, G. (2015) Novel microfluidics approach for extremely fast and efficient photochemical transformations in fluoropolymer microcapillary films. ChemicalCommunications 51, 8414–8417.

Richardson, S.D. (2012) Environmental mass spectrometry: emerging contaminants and current issues. Analytical Chemistry 84, 747–778.

Richardson, S.D., Plewa, M.J.,Wagner, E.D., Schoeny, R., DeMarini, D.M. (2007) Occurrence, genotoxicity, and carcinogenicity of regulated and emerging disinfection by-products in drinking water: a review and roadmap for research. Mutation Research 636(1-3), 178-242.

Rozas, O., Vidal, C., Baeza, C., Jardim, W.F., Rossner, A., Mansilla, H.D. (2016) Organic micropollutants (OMPs) in natural waters: Oxidation by UV/H_2O_2 treatment and toxicity assessment. Water Research 98, 109–118.

Russo, D., Spasiano, D., Vaccaro, M., Andreozzi, R., Li Puma, G., Reis, N.M., Marotta, R. (2016) Direct photolysis of benzoylecgonine under UV irradiation at 254 nm in a continuous flow microcapillary array photoreactor. Chemical Engineering Journal 283, 243–250.

Sanderson, H., Johnson, D.J., Reitsma, T., Brain, R.A., Wilson, C.J., Solomon, K.R. (2004) Ranking and prioritization of environmental risks of pharmaceuticals in surface waters. Regulatory Toxicology and Pharmacology 39(2), 158–183.

Shi, P., Jia, S., Zhang, X.X., Zhang, T., Cheng, S., Li, A. (2013) Metagenomic insights into chlorination effects on microbial antibiotic resistance in drinking water. Water Research 47, 111–120.

Singer, A.C., Nunn, M.A., Gould, E.A., Johnson, A.C. (2007) Potential risks associated with the proposed widespread use of Tamiflu. Environmental Health Perspectives 115(1), 102–106.

Sinha, V.R., Monika, Trehan, A., Kumar, M., Singh, S., Bhinge, J.R. (2007) Stress studies on Acyclovir. Journal of Chromatographic Science 45, 319–324.

Spasiano, D., Russo, D., Vaccaro, M., Siciliano, A., Marotta, R., Guida, M., Reis, N.M., Li Puma, G., Andreozzi, R. (2016) Removal of benzoylecgonine from water matrices through UV_{254}/H_2O_2 process: reaction kinetic modeling, ecotoxicity and genotoxicity assessment. Journal of Hazardous Materials 318, 515–525.

Yuan, F., Hu, C., Hu, X., Wei, D., Chen, Y., Qu, J. (2011) Photodegradation and toxicity changes of antibiotics in UV and UV/H_2O_2 process. Journal of Hazardous Materials 185, 1256–1263.

673 Zhou, C., Chen, J., Xie, Q., Wei, X., Zhang, Y., Fu, Z. (2015) Photolysis of three antiviral drugs
674 acyclovir, zidovudine and lamivudine in surface freshwater and seawater. Chemosphere 138, 792–
675 797.

Figure 1: Comparison between experimental (circle) and predicted (line) data for UV_{254} photolysis of ACY at different pH and power of lamp in the MCF photoreactor.

(a) pH = 6.0 **(**8.0 W); **(b)** pH = 4.0 **(**8.0 W**); (c,d)** pH = 6.0 **(**4.5 W**); (e)** pH = 8.5 **(**8.0 W**).**

Figure 2: Comparison between experimental (circle) and predicted (line) data for UV_{254}/H_2O_2 photodegradation of ACY (●) and hydrogen peroxide (○) in the MCF photoreactor at different pH, power of lamp and starting H_2O_2 load. *Optimization mode* (**a-f**), *simulation mode* (**g-m**).

(a): pH = 6.0 (8.0 W, $[H_2O_2]_o/[ACY]_o$ = 20); **(b):** pH = 6.0 (8.0 W, $[H_2O_2]_o/[ACY]_o$ = 50);

(c): pH = 8.0 (8.0 W, $[H_2O_2]_o/[ACY]_o$ = 50); **(d):** pH = 6.0 (4.5 W, $[H_2O_2]_o/[ACY]_o$ = 50);

(e): pH = 6.0 (4.5 W, $[H_2O_2]_o/[ACY]_o$ = 70); **(f):** pH = 6.0 (4.5 W, $[H_2O_2]_o/[ACY]_o$ = 100);

(g): pH = 4.0 (8.0 W, $[H_2O_2]_o/[ACY]_o$ = 100); **(h):** pH = 8.2 (8.0 W, $[H_2O_2]_o/[ACY]_o$ = 100);

(i): pH = 4.0 (4.5 W, $[H_2O_2]_o/[ACY]_o$ = 20); **(l) pH = 6.0 (8.0 W, $[H_2O_2]_o/[ACY]_o$ = 60);**

(m) pH = 6.0 (8.0 W, $[H_2O_2]_o/[ACY]_o$ = 142).

Figure 3: Evolution of acute toxicity with *D. magna* (24 h and 48h) during the UV_{254} (**A**) and UV_{254}/H_2O_2 (**B**) treatments. Data with different letters (a-b) are significantly different (Tukey's, $p<0.05$).

Figure 4: Toxicity data with *R. subcapitata* (72 h). Data with different letters (a–c) are significantly different (Tukey's, $p<0.05$).

Figure 5: Effects of UV_{254} and UV_{254}/H_2O_2 processes on (A) ROS production, (B) SOD, (C) Cat, (D) GST in *Daphnia magna* after 48 h of exposure. For each parameter, mean and standard deviation are shown. Data with different letters (a-d) are significantly different (Tukey's, $p<0.05$). *Ctr- (negative control)

Figure 6: Survival curves of *D. magna* during the time of exposure (21 days) for UV_{254} (**A**) and UV_{254}/H_2O_2 (**B**) treated solutions. Data with different letters (a-b) are significantly different (Tukey's, $p<0.05$). Dilution: 1:100.

Table 1: Occurrence of ACY in WWTP effluents and in surface waters.

Table 2: Reaction kinetics mechanism of ACY photoxidation by UV_{254}/H_2O_2 process and mass balance equations. The terms $f_{H_2O_2}$ and f_{ACY} indicate the fraction of UV_{254} radiation absorbed by hydrogen peroxide and ACY respectively. The TPs concentration was assumed equal to the amount of ACY consumed ($[ACY]_0 - [ACY]$).

ε_{254}^{H2O2} and ϕ_{H2O2} are the molar absorption coefficient and the quantum yield of photolysis of for hydrogen peroxide at 254 nm respectively.

Table 3: First brood and live offspring after 21 days of *D. magna* exposure for different UV_{254} doses (with and without hydrogen peroxide).

Table 4: Molecular structures of the chemical species identified from the MS spectra of samples submitted to UV_{254} and UV_{254}/H_2O_2 photolysis.

(°) The structures proposed on the basis of the pseudo-molecular $[M+H]^+$ ion due to the low intensity of the MS/MS fragmentation signals.

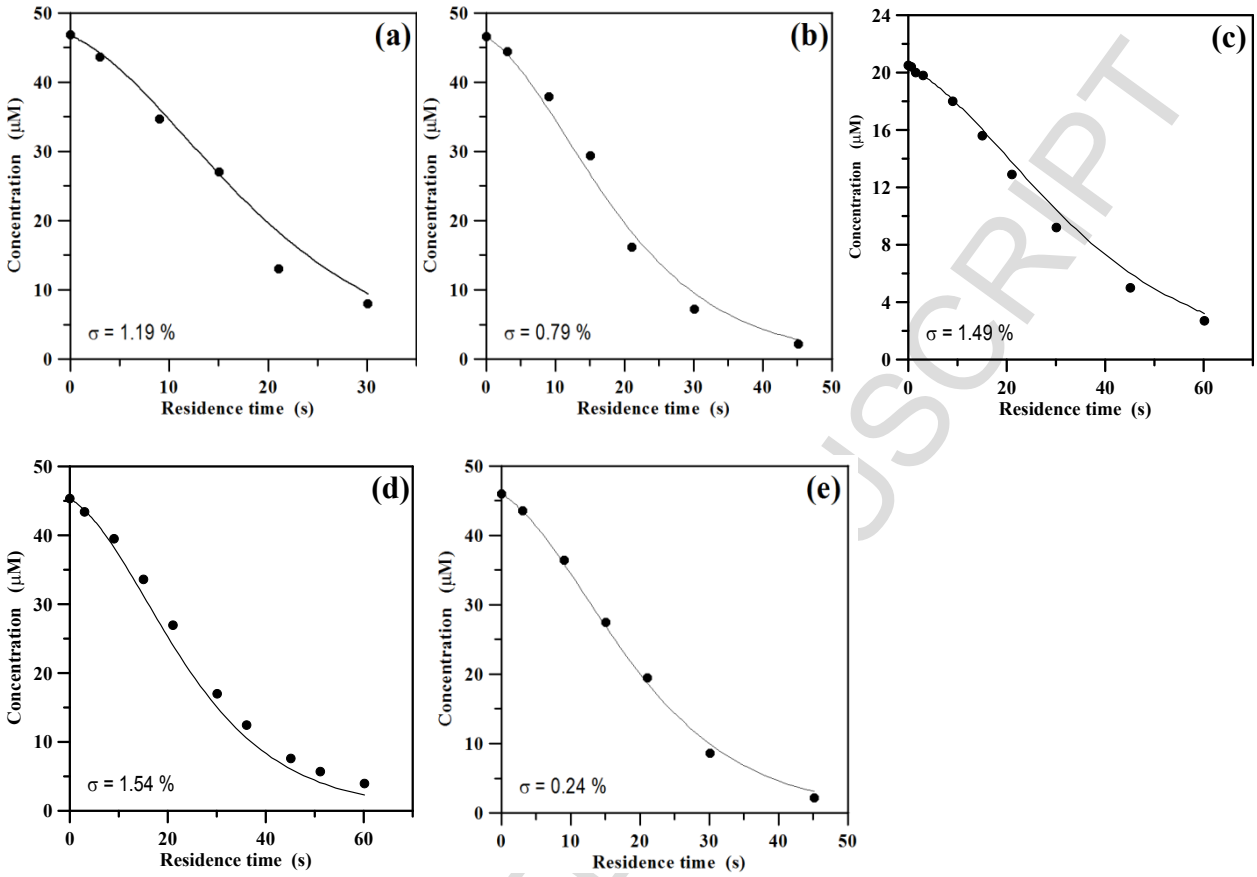

Figure 1

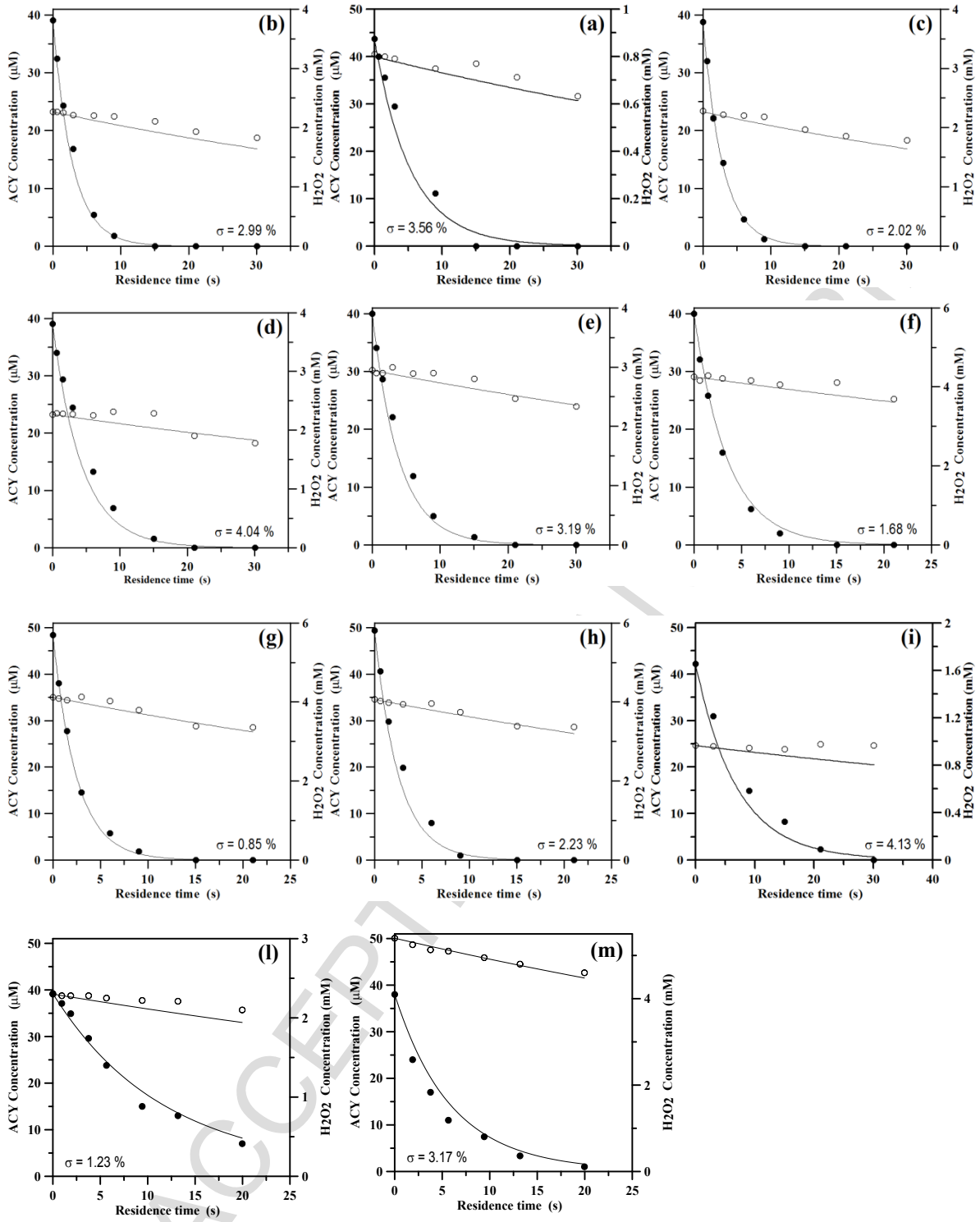
(a)
σ = 3.56 %
(b)
σ = 2.99 %
(c)
σ = 2.02 %
(d)
σ = 4.04 %
(e)
σ = 3.19 %
(f)
σ = 1.68 %
(g)
σ = 0.85 %
(h)
σ = 2.23 %
(i)
σ = 4.13 %
(l)
σ = 1.23 %
(m)
σ = 3.17 %
ACY Concentration (μM)
H2O2 Concentration (mM)
Residence time (s)

Figure 2

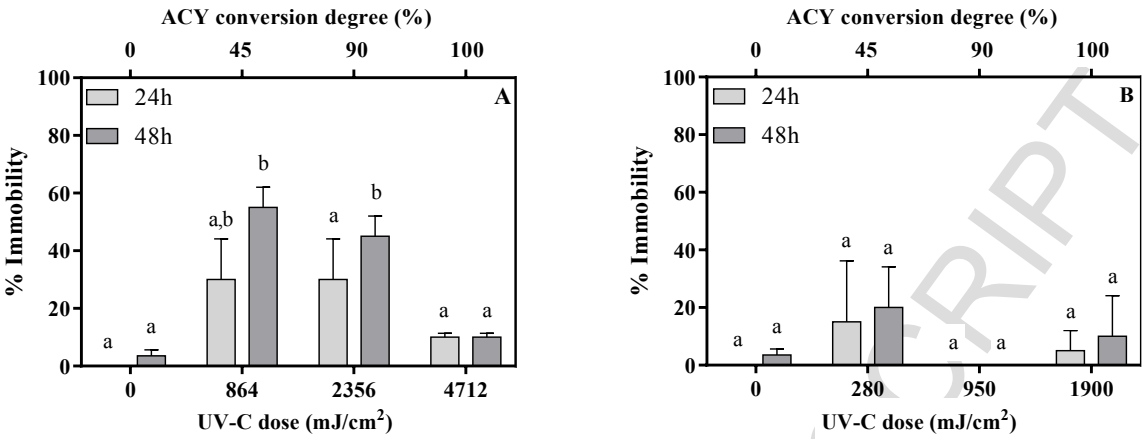

Figure 3

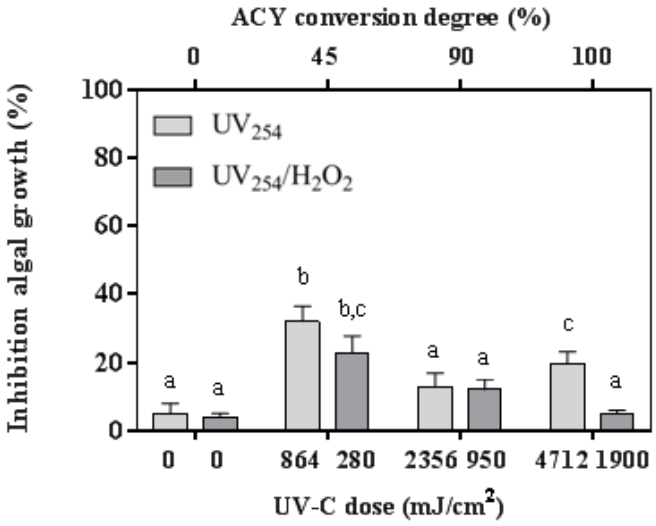

Figure 4

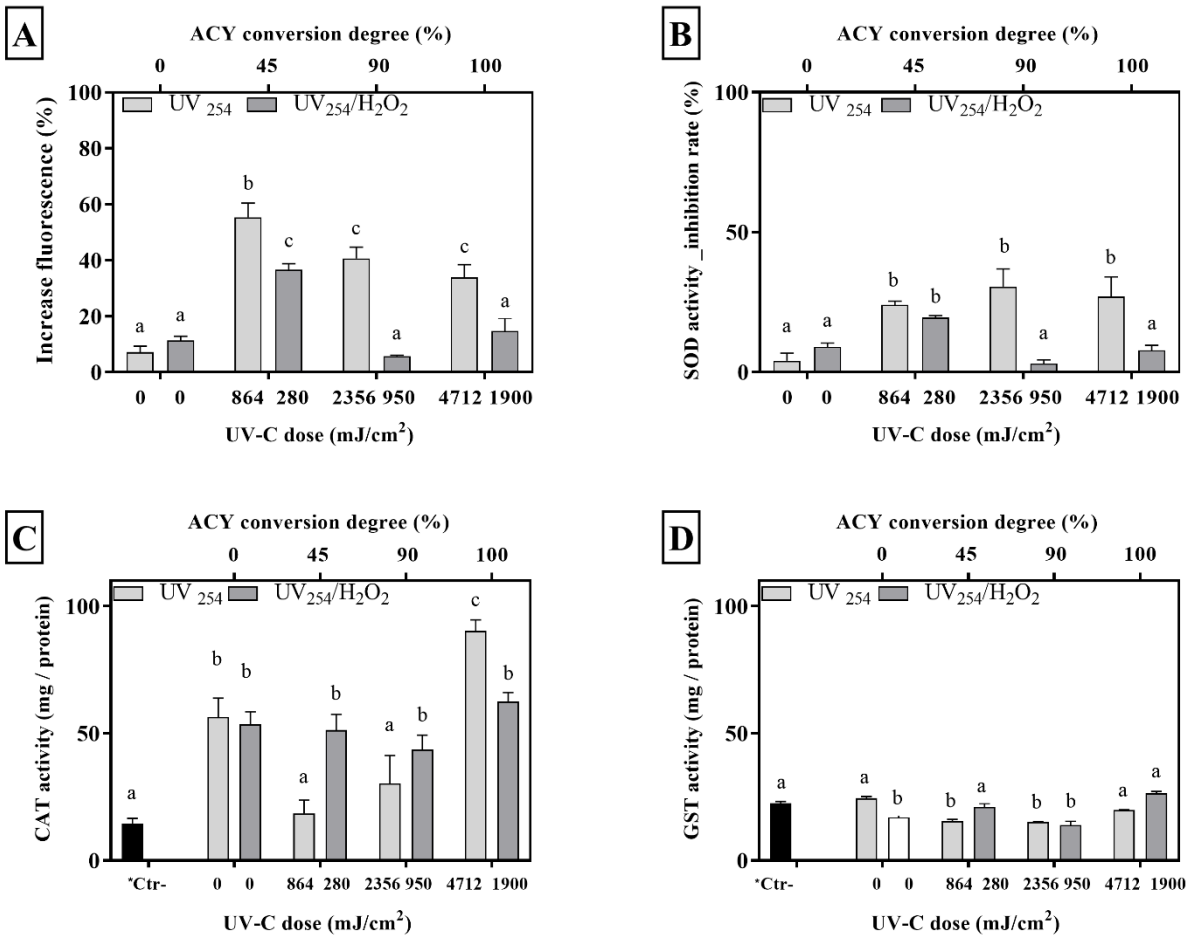

Figure 5

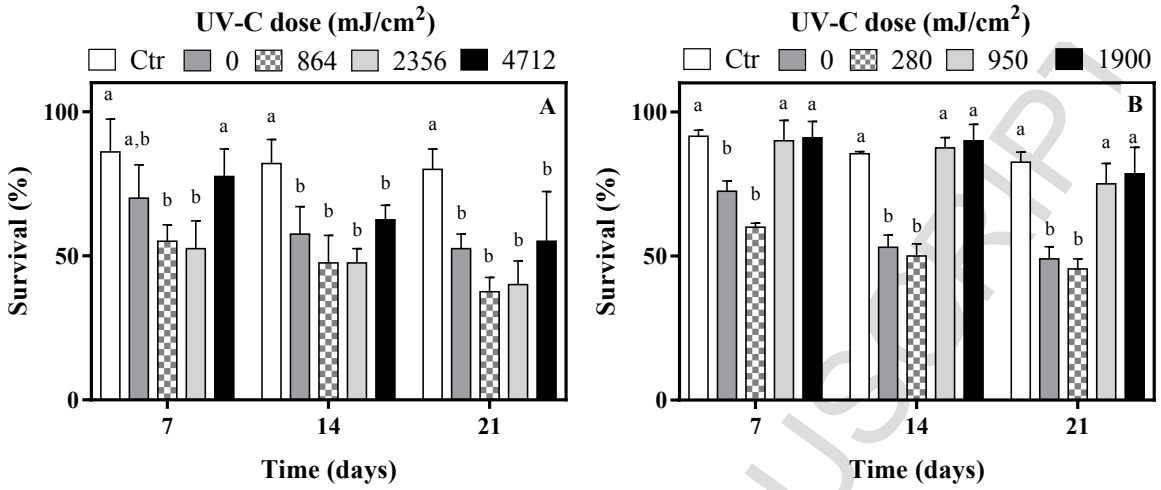

Figure 6

- Photolysis and UV/H_2O_2 degradation of acyclovir were studied in a microphotoreactor
- UV_{254} photolysis quantum yield of acyclovir was estimated ($1.62 \cdot 10^{-3}$ mol·ein^{-1})
- Kinetic constant of hydroxyl radical attack to acyclovir was evaluated
- H_2O_2 assisted photo-oxidation process reduces the ecotoxicity of acyclovir

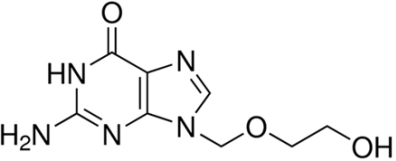

Acyclovir

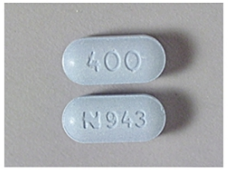

UV_{254} lamps

Kinetics

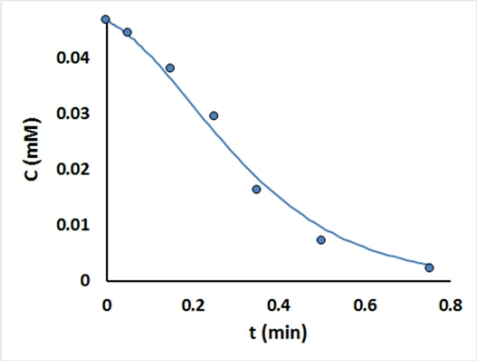

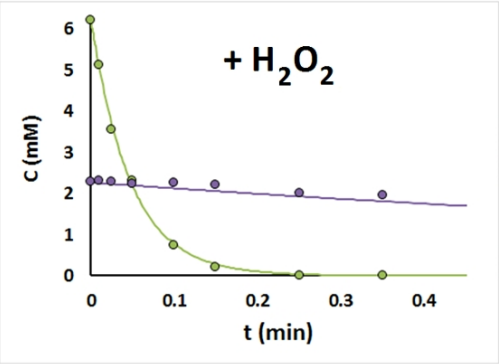

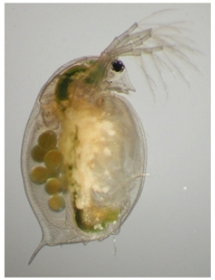

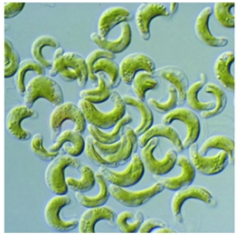

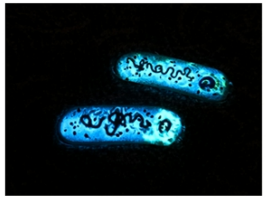

Ecotoxicity

WWTP effluent (ng/L)	Surface water (ng/L)	Location	Ref
27.3 – 53.3	2.2 - 190	Germany	(Prasse et al., 2010)
121- 148	5 - 25	Germany	(Prasse et al., 2011)
44.0 - 650	--	Germany	(Funke et al., 2016)
114 - 205	8.9 – 112.6	China	(Peng et al., 2014)
12 - 50	10 - 23	Japan	(Azuma et al., 2016)
947	738 - 1590	USA	(Bradley et al., 2014)
154	--	USA	(McCurry et al., 2014)

Table 1

3)	$\mathrm{ACY} \xrightarrow{h\nu} \mathrm{TPs}$	$\emptyset_{ACY}$	(estimated in this study)
4)	$\mathrm{H_2O_2} \xrightarrow{h\nu} 2\mathrm{HO}^{\bullet}$	$\emptyset_{H_2O_2} = 0.55\ mol{\cdot}ein^{-1}$ $\varepsilon_{254}^{H_2O_2} = 18.6\ M^{-1}{\cdot}cm^{-1}$	(Goldstein et al., 2007)
5)	$\mathrm{HO}^{\bullet} + \mathrm{H_2O_2} \xrightarrow{k_h} \mathrm{H_2O} + \mathrm{HO_2^{\bullet}}$	$k_h = 2.7 \cdot 10^7 M^{-1}{\cdot}s^{-1}$	(Buxton et al., 1988)
6)	$\mathrm{ACY} + \mathrm{HO}^{\bullet} \xrightarrow{k_{OH/ACY}} \mathrm{TPs}$	$k_{OH/ACY}$	(estimated in this study)
7)	$\mathrm{TPs} + \mathrm{HO}^{\bullet} \xrightarrow{k_{OH/TP}} \mathrm{TP}$	$k_{OH/TP}$	(estimated in this study)
8)	$2\mathrm{HO_2^{\bullet}} \xrightarrow{k_t} \mathrm{H_2O_2} + \mathrm{O_2}$	$k_t = 8.3 \cdot 10^5\ M^{-1}{\cdot}s^{-1}$	(Bielski et al., 1985)

9) $$\frac{d[HO^{\bullet}]}{d\tau} = 2F_{H_2O_2} - [HO^{\bullet}] \cdot \left(k_h \cdot [H_2O_2] - k_{OH/ACY} \cdot [ACY] - k_{OH/TP} \cdot [TPs]\right)$$

10) $$F_{H_2O_2} = \emptyset_{H_2O_2} \cdot P_o \cdot \left(1 - exp\left(-2.3 \cdot l_{MCF} \cdot \left(\varepsilon_{254}^{ACY} \cdot [ACY] + \varepsilon_{254}^{H_2O_2} \cdot [H_2O_2]\right)\right)\right) \cdot f_{H_2O_2}$$

11) $$\frac{d[HO_2^{\bullet}]}{d\tau} = k_h \cdot [HO^{\bullet}] \cdot [H_2O_2] - 2k_t \cdot [HO_2^{\bullet}]^2$$

12) $$\frac{d[ACY]}{d\tau} = -F_{ACY} - k_{OH/ACY} \cdot [ACY] \cdot [HO^{\bullet}]$$

13) $$F_{ACY} = \emptyset_{ACY} \cdot P_o \cdot \left(1 - exp\left(-2.3 \cdot l_{MCF} \cdot \left(\varepsilon_{254}^{ACY} \cdot [ACY] + \varepsilon_{254}^{H_2O_2} \cdot [H_2O_2]\right)\right)\right) \cdot f_{ACY}$$

Table 2

UV_{254}		
Sample	First brood (day)	Number of Living offspring per parent animal
Control solution	8	78 ± 5
UV_{254} dose: 0 mJ·cm^{-2}	10	72 ± 3
UV_{254} dose: 864 mJ·cm^{-2} **TOC removal degree: < 5%**	15	42 ± 3
UV_{254} dose: 2356 mJ·cm^{-2} **TOC removal degree: < 5%**	17	37 ± 6
UV_{254} dose: 4712 mJ·cm^{-2} **TOC removal degree: ~ 5%**	11	68 ± 5
UV_{254}/H_2O_2		
Sample	First brood (day)	Number of Living offspring per parent animal
Control solution	8	75 ± 1
UV_{254} dose: 0 mJ·cm^{-2}	10	74 ± 4
UV_{254} dose: 280 mJ·cm^{-2} **TOC removal degree: 28 %**	9	69 ± 5
UV_{254} dose: 950 mJ·cm^{-2} **TOC removal degree: 77 %**	9	65 ± 2
UV_{254} dose: 1900 mJ·cm^{-2} **TOC removal degree: > 95 %**	9	70 ± 2

Table 3

n°	Previously reported	Measured mass $[M+H]^+$ (Da)	Structure (°)
		UV_{254}	
I	NO	136.93	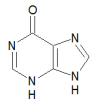
II	*YES, An et al, 2015*	158.15	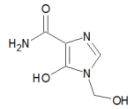
III	NO	202.18	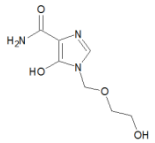
IV	*YES, An et al, 2015*	242.98	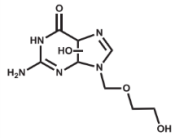
V	*YES, An et al, 2015*	258.98	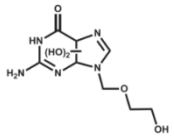
		UV_{254}/H_2O_2	
VI	NO	103.08	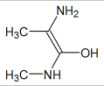
VII	*YES, Iqbal et al., 2005*	113.07	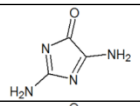
VIII	NO	129.07	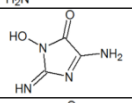
IX	NO	146.09	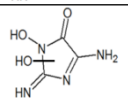
X	*YES, Iqbal et al., 2005*	156.08	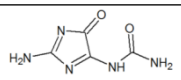
XI	NO	214.17	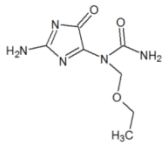
VI	NO	230.12	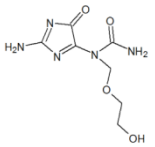

Table 4